AIAA-2002-5272

Plasma formation during high speed flights in upper layers of the Earth's atmosphere.

S. Mazouffre, V. Lago, M. Lino da Silva, and M. Dudeck
Laboratoire d'Aérothermique, CNRS, 1C avenue de la Recherche Scientifique, 45071 Orléans, France.

E. Pawelec
University of Opole, Oleska 48, Opole, Poland.

11th AIAA/AAAF International Conference
Space Plane and Hypersonic Systems and Technologies
29 september-4 October 2002
Orléans, France

PLASMA FORMATION DURING HIGH SPEED FLIGHTS IN UPPER LAYERS OF THE EARTH'S ATMOSPHERE.

S. Mazouffre[†], E. Pawelec[‡], V. Lago[†], M. da Silva[†], and M. Dudeck[†]

Abstract

A flight at supersonic speeds in the Earth's atmosphere leads to the appearance of a plasma that surrounds the vehicle. This well-known phenomenon finds its origin in the existence of a bow shock wave that must be regarded as the plasma source. In this paper, only flights at relatively high altitude, i.e. in a low pressure environment, are considered. After explaining in detail the mechanism responsible for the plasma formation, we discuss ground simulation of supersonic flight conditions by means of rarefied supersonic plasma jets. The present-day ground test facility of the Laboratoire d'Aérothermique, the so-called SR5 plasma wind-tunnel, is presented here together with the set of diagnostic tools employed to characterise the plasma flow. Both the dynamics and chemistry of free air plasma jets are described. In the final section, a set of recent results that concern the interaction between a supersonic plasma jet and a metal object is presented.

Introduction

To address the problem of plasma formation during a high speed flight in upper layers of the Earth's atmosphere is challenging. Indeed, in addition to a very complex chemistry and departure from thermodynamic equilibrium, rarefied hypersonic flow conditions and interactions between the plasma and the surface of the vehicle have to be considered. Nevertheless, the improvement in the understanding of the physics of such a plasma medium has a direct impact on several points: The optimisation of the vehicle's thermal shield, the determination of the plasma frequency which drives attenuations in radio transmissions and the black-out phenomenon, the possibility of modifying the plasma properties for camouflage and lure effects (EM signature). Moreover, the created plasma also plays a role in the overall flight dynamics.

Shock wave and plasma formation

In the course of a supersonic/hypersonic flight in the upper layers of the Earth's atmosphere, the vehicle, e.g. plane, ballistic missile, spacecraft, is surrounded by a plasma, i.e. an ionised gas. The plasma formation is a direct consequence of conversion of kinetic energy of the vehicle into thermal and internal energy of the surrounding medium. In Fig. 1, an example of the evolution of speed and Mach number as a function of the altitude that can be reached during an earth entry is shown. The very high speed of the vehicle is responsible for the appearance of a strong compression shock wave in front of the latter. The bow shock wave is a zone through which energy is dissipated whereas the flow passes from a supersonic to a subsonic regime. The plasma is formed within the shock wave, as soon as the temperature resulting from the deceleration-compression effect is high enough to allow excitation of the gas molecule internal energy modes (electronic, vibration, rotation) up to the point where dissociation and ionisation reactions occur. Electrons resulting from collision between heavy particles participate in turn to the plasma production process, especially to the ionisation process for which an avalanche effect is quickly initiated. Hence, the bow shock wave corresponds to the main zone of plasma formation (plasma production also occurs behind the shock where the temperature is still high). The bow shock can be considered as the plasma precursor. Note that light emitted by the plasma, which originates in relaxation and momentum transfer processes (line and continuum radiation), can in turn influence the shock wave characteristics due to the radiation pressure.

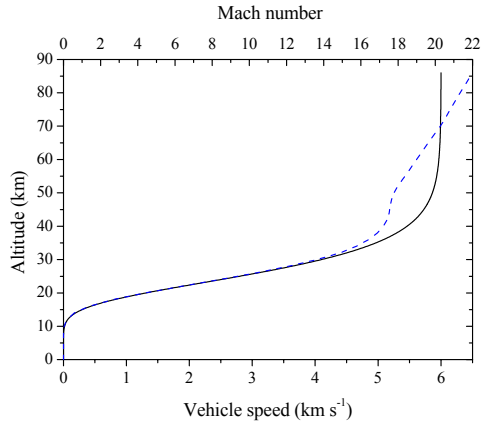

Fig. 1: Trajectory for an earth entry with: 6 km/s at 86 km, entry angle of 10°, 1 m vehicle length, 1000 kg weight (solid line). Corresponding Mach number calculated from the local speed of sound (dashed line).

The created plasma is therefore a medium of complex chemistry, due to the presence of neutrals, ions, electrons, atomic radicals, molecular

[†] Laboratoire d'Aérothermique, CNRS, 1C avenue de la Recherche Scientifique, 45071 Orléans, France.
[†] University of Opole, Oleska 48, Opole, Poland.

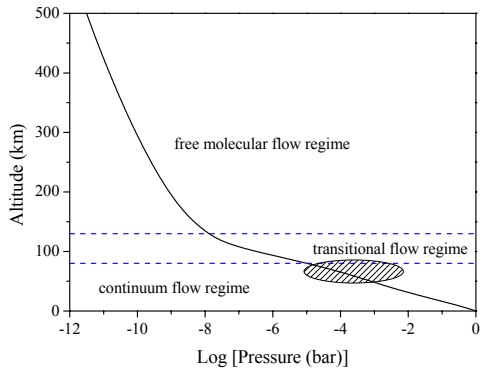

Fig. 2: Pressure as a function of the altitude for the 1976 US standard atmosphere. Also shown are the three different flow regimes (for a characteristic length of 1 m). The hatched area corresponds to the domain of ground simulation of the Laboratoire d'Aérothermique.

fragments and photons, of which the existence cannot be ignored. The plasma that appears during supersonic flights is weakly ionised (the charged particle fraction is usually below 1%) and strongly dissociated. In the post-shock region, the flow reaches a state of thermodynamic non-equilibrium, as one temperature is no longer enough to characterise the medium. Moreover, in this region a departure from Maxwellian energy distribution is possible.

Many hypersonic flights taking place in the upper layers of the atmosphere (such as space re-entry flights), it is important to determine the flow regime since the latter varies with the altitude, as shown in Fig. 2. The flow regime is determined according to the magnitude of the dimensionless Knudsen number Kn, which is the ratio of the particle mean free path to a characteristic length scale of the system. If $Kn < 0.01$ then the flow is said to be in hydrodynamic regime and the continuum model is applicable (Navier-Stokes equation sets). For $0.01 < Kn < 0.1$, the flow is in a transition regime but it can still be treated as a continuum medium, except in the boundary layer. Finally, for $Kn > 0.1$, the flow enters the free molecular regime and one must refer to the molecular dynamic theory (use of statistical methods such as Direct Simulation Monte-Carlo to characterise the flow). During earth entries depending on the velocity (6 to 12 $km.s^{-1}$) plasma effects start to be noticeable at about 100 km altitude, i.e. in the transitional flow domain, as can be seen in Fig. 2. Typically, plasma effects must be taken into account down to 60 km. At lower altitude, the pressure is sufficient to maintain a low electron density, and hydrodynamic effects like heat transfer and turbulence are dominant.

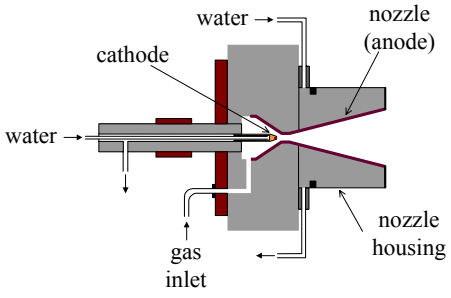

Fig. 3: Simplified drawing of the vortex-stabilised dc-arc torch equipped with a convergent-divergent nozzle.

Rarefied supersonic plasma jet as a simulation tool

At the Laboratoire d'Aérothermique in Orléans, low pressure supersonic flight conditions in the Earth's atmosphere are simulated using rarefied supersonic plasma jets, also called free plasma jets. The ground-test facility currently in operation in Orléans is named the SR5 wind-tunnel.

The SR5 plasma wind-tunnel

The plasma source used in the ground-test facility is a vortex stabilised dc-arc torch [1]. It is schematically depicted in Fig. 3. The torch is equipped with a flat zirconium cathode and with a convergent (60°)-divergent (30°) copper nozzle that acts as a grounded anode. Both the cathode and the anode are water-cooled. The torch can be operated in a wide range of currents (50 to 200 A) and flows (5 to 40 slm). The global efficiency is around 50%. The plasma torch can be operated for several hours, the lifetime being determined by the cathode erosion. The gas is fed through a mass flow controller into the cathode area (side injection). The torch is mounted on a moveable arm and can therefore be moved in vertical and horizontal direction. A thermal plasma is created in either a N_2-O_2 gas mixture or directly in air at the cathode

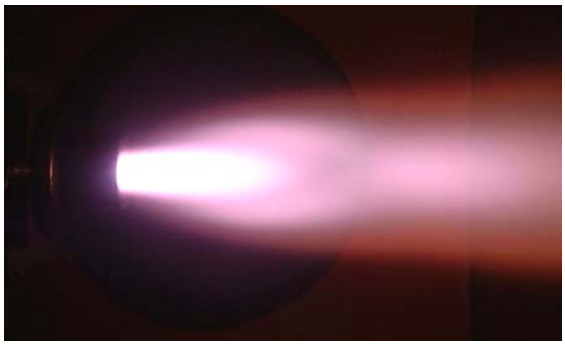

Fig. 4: Photograph of a free argon plasma jet (60 A, 44 V, 30 Pa background pressure). The jet structure and boundary are clearly visible. The dark zone at the jet centre corresponds to the zone of silence; it is located just ahead of the normal stationary shock wave. The red colour visible at the jet boundary is a sign for air drag (continuous release of a minute amount of air in the vessel).

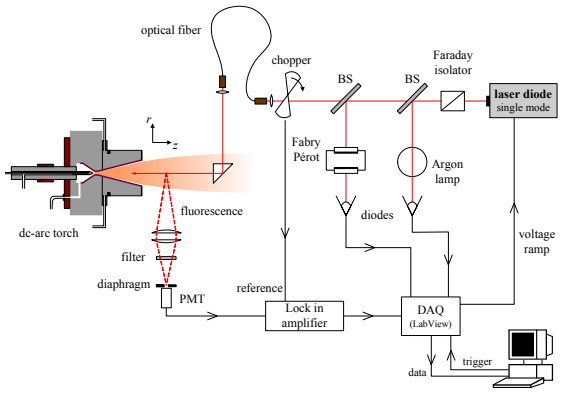

Fig. 5: Schematic view of the experimental LIF setup using a cw laser source and synchronic detection (in parallel configuration). Spatially resolved measurements are realized by moving the plasma torch.

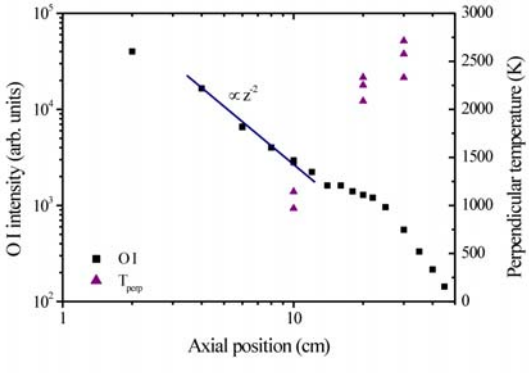

Fig. 6: Axial profile of the light intensity of the 777 nm O I line for p_{back} = 4 Pa (square). In the supersonic domain, the density decreases as z^{-2} owing to the rarefaction effect (frozen chemistry). Perpendicular temperature jump across the normal shock wave of an Ar-N_2 plasma jet (70 A) measured by means of cw-LIF at p_{back} = 4 Pa (triangle).

throat (4 mm diameter). The generated plasma is characterised by a relatively high gas pressure (about 0.5 atm), high electron and heavy particle temperatures both around 1 eV and a high ionisation degree estimated to be around 10%.

Subsequently the plasma expands freely from the torch nozzle into a low pressure vessel made of steel. The vacuum chamber is 4.3 m long and has a diameter of 1.1 m. The pumping capacity can be varied by means of a valve, and in this way the residual pressure can be changed from 1 Pa to 10^4 Pa almost independently from the gas flow.

The expansion of the plasma into a low-pressure chamber (typically 10 Pa), i.e. the formation of a free plasma jet, allows the plasma to reach hypersonic speed (Mach number M up to 8) at low pressure. Objects with various geometries can be inserted into the plasma jet; and subsequently a shock wave is formed around them. In this way, one can approach conditions encountered during high speed flight in upper layers of the Earth's atmosphere. This kind of plasma wind-tunnel offers two advantages: the easiness of probing the jet owing to its large size, and stationary flow conditions. Studies performed in Orléans are complementary to studies performed in Marseille (IUSTI) with the TCM2 shock tube (M up to 20) and in Toulouse (ONERA) with the F4 pulsed hypersonic wind-tunnels (M up to 20).

In Fig. 4, a photograph of a free argon plasma jet, taken with an ordinary digital camera without filter, is shown. The jet structure (see next section) and boundary are clearly visible.

Set of diagnostic tools

The SR5 plasma wind-tunnel is equipped with various diagnostic tools: electrostatic probes to determine electronic properties like n_e and T_e and to measure the flow velocity, mass spectrometer to obtain the plasma composition, and emission spectrometer to monitor the light emitted by excited atoms and molecules. Two complementary techniques are currently being implemented: Fabry-Pérot interferometry and Laser Induced Fluorescence (LIF) spectroscopy [2] in order to be able to locally measure the plasma velocity (r and z components) and translational temperature (perpendicular and parallel components). The large set of collected data allows studying the free plasma jet flow pattern, the stationary shock front features as well as the plasma chemistry. When a body is placed into the jet, the zones of special interest are the bow shock wave, the thermal and the chemical boundary layers and the wake.

A schematic view of the cw LIF setup is depicted in Fig 5. Preliminary measurements have been performed with an Ar-N_2 mixture (70 A, 4 Pa) in order to test and to optimise the setup. The perpendicular temperature, associated with the

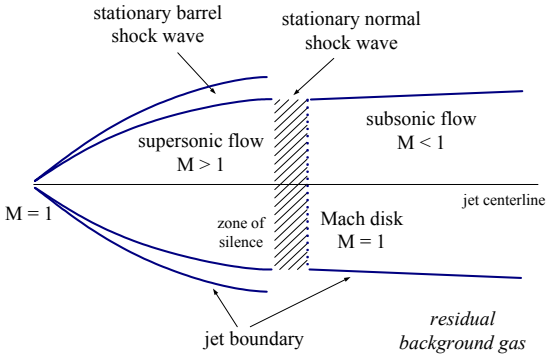

Fig. 7 : Simplified structure of a free plasma jet. The plasma first expands supersonically. At some distance from the source a normal shock wave is formed. Behind the shock front the plasma flows subsonically and at constant static pressure. The supersonic flow domain is limited by a barrel (side) shock wave. M refers to the Mach number.

velocity distribution function perpendicular to a streamline, of metastable Ar atoms has been measured along the jet axis within the normal stationary shock wave that results from interaction between the jet and the residual background gas (see next section). Results are shown in Fig. 6. From the magnitude of the observed temperature jump and using the Rankine-Hugoniot relations, the Mach number ahead of the shock wave can be estimated: One finds M≈3. Assuming that the speed of sound is close to the local thermal speed, one can also estimate the gas velocity ahead of the shock wave: One finds v≈2 km.s^{-1}. Those results are only preliminary and they are certainly underestimated. They should be considered as a lower linit.

Supersonic plasma jet characteristics

A detailed description of the physics of free plasma jets can be found elsewhere [3,4]. Here only a short overview of the expansion picture is presented. Because the plasma expands through a nozzle from a high pressure region into a low pressure region, a well-defined free jet shock wave structure is produced, as depicted in Fig. 7. The plasma first flows supersonically, as can be seen in Fig. 8 (in Orléans, M=1 at the nozzle throat and the flow is already supersonic in the divergent section). In this flow domain, the drift velocity increases and due to energy conservation the temperature drops in accordance with the Poisson adiabatic law, as shown in Fig.9. Figures 8 and 9 correspond to measurements realised at the Eindhoven University of Technology in the Netherlands. Flow characteristic of ground-state nitrogen atoms in a nitrogen plasma jet generated by a cascaded arc has been studied by means of Two-photon Absorption Laser Induced Fluorescence (TALIF) spectroscopy [5]. In the mean time, the particle density along a streamline decreases because of the increase in the jet diameter (rarefaction effect). At some distance from the source, depending on the source stagnation pressure and on the background pressure, a normal stationary shock wave is formed to allow the flow to adapt to the ambient gas conditions. The shock wave originates in the direct interaction, i.e. collision, between the supersonic jet and the residual background gas. The Mach disk, location at which the Mach number equals 1, defines the end of the shock wave. Throughout the shock region, of which dimensions are in the order of the local neutral-neutral collision mean free path (in Fig. 6 the shock front thickness is around 20 cm), the flow undergoes a transition from a supersonic regime to a subsonic regime. The flow is strongly decelerated across the shock wave (see Fig. 8). As a consequence, the temperature increases because of energy conservation (see Fig. 9), and the density increases (compression effect due to momentum conservation). Behind the shock wave, the plasma

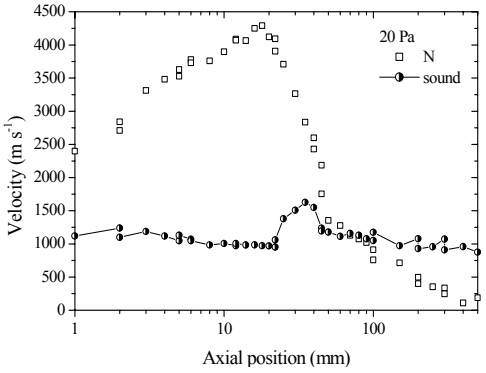

Fig. 8: Development of the N atom axial velocity component along the plasma jet centerline. Also shown is the speed of sound calculated from the measured parallel temperature. The Mach number M equals 4.4 ahead of the shock front.

flows subsonically and at constant static pressure. The supersonic domain is surrounded by a so-called stationary barrel shock wave. When the background pressure is such that Kn≈1, the shock structure is absent and a supersonic plasma beam, collisionless flow, is created.

Deviation from the classical free jet flow picture (expansion of a hot neutral gas) may appear in the case of transient species. For ions and electrons, recombination reactions, the long range Coulomb interaction, and charge exchange processes must be considered [4,6]. It has recently been demonstrated that the transport of atomic radicals like H atoms [4,7] and N atoms [5] in supersonic plasma jets is strongly influenced by surface chemistry.

Excited oxygen atoms

In Fig. 6, the axial profile of the light intensity of the 777.2 nm O I line is shown for an air plasma jet. This profile corresponds to the relative axial density

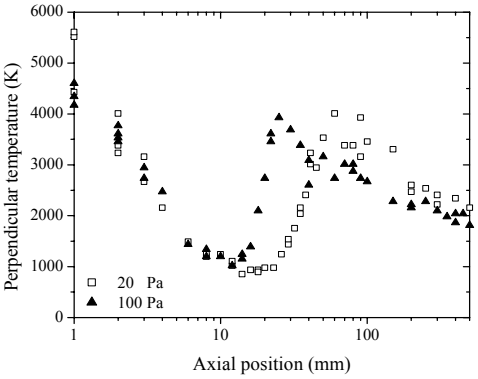

Fig. 9: Profile of the N atom perpendicular temperature along the plasma jet axis at 20 Pa and 100 Pa background pressure. The effect of p_{back} upon both the shock wave position and thickness is clearly visible.

profile of the O ($3p^5P_3$) resonant state (small light integration path in comparison with the jet radius). The O resonant state is locally produced, in view of its short radiative lifetime (few ns). At low pressure, one may consider two production routes: Recombination of atomic oxygen ion or dissociative recombination of O containing molecular ions. In the supersonic domain, the density decreases as z^{-2} owing to the rarefaction effect. Note that this is a sign for a frozen chemistry. There is obviously no density jump across the shock wave, contrary to expectation. There may be several reasons: Weak source term due to appearance of parallel chemical reactions, direct losses (outward diffusion) driven by density gradients [4,5]. The fast density drop in the subsonic domain may be understood in term of a low charge particle content.

Chemistry of air plasma jets

The chemistry of the plasma formed behind a shock wave surrounding an object flying in the Earth's atmosphere has been studied intensely since the 60s [8], both on a theoretical and numerical point of view as well as on an experimental point of view mainly with shock tube experiments [9]. Here we briefly summarise the main outcomes of 40 years of investigations that concern the appearance of a weakly ionised plasma in a bow shock before focusing onto the specific chemistry of rarefied supersonic air plasma jets employed in Orléans.

Within a bow shock wave

In addition to dry air composed of 78.08 % N_2, 20.95 % O_2, 0.93 % Ar and several other gases, the Earth's atmosphere contains a non-negligible amount of water molecules which play an important role in the overall plasma generation scheme.
N_2 and O_2 molecules, the dominant species, are first dissociated within and behind the shock wave where the heavy particle temperature reaches several thousands of K. Electrons are first produced by the associative-ionisation reaction $N + O \rightarrow NO^+ + e$. This reaction is followed by several charge-exchange reactions, which lead to the production of NO and numerous atomic and molecular ions [8]. When the electron density reaches a given threshold, ions are produced via direct electron impact with N and O atoms and an avalanche effect is started. A detailed review of the chemistry and kinetics of air plasmas can be found in references [8,10]. Several dissociation and ionisation models for air at hypersonic speed are examined in [11]. Water dissociation models at high altitude for OH production are discussed in [12]. For information the dissociation and ionisation energy of main compounds encountered in air plasmas are given in Fig. 10.

Species	E dissociation in eV	E ionisation in eV
N_2	9.8	15.6
O_2	5.1	12.1
NO	6.5	9.1
OH	4.6	13.0
N	-	14.5
O	-	13.6
H	-	13.6
Ar	-	15.8

Fig. 10: Dissociation and ionisation energy of main compounds encountered in air plasmas (1 eV corresponds to 11600 K)

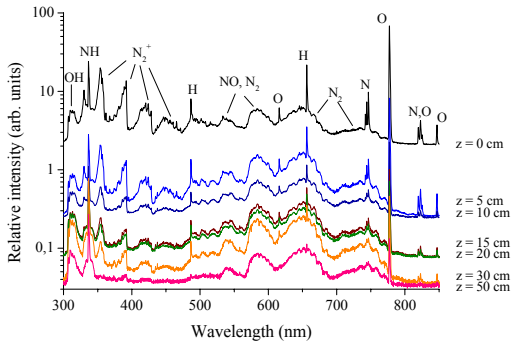

Fig. 11: Raw emission spectrum of an air plasma jet obtained for several positions along the axis (160 A, 6.7 Pa). All atomic peaks and molecular bands are identified.

Plasma jet: light emission analysis

Emission spectroscopy allows in a non-intrusive way to identify and to quantify excited species present in the plasma. The light emitted by a supersonic air plasma jet has been analysed in the range 300-850 nm using a pocket monochromator equipped with a CCD camera and an optical fiber (Avantes AVS-USB2000, 1 nm resolution).
In Fig. 11, one can see raw emission spectrum of an air plasma jet obtained for several positions along the centreline. The plasma contains atomic radicals like H, N and O, N_2 molecules and molecular fragments like OH, NH and NO. O_2 cannot be observed here due to a weak emission in the visible range but the strong Schumann-Runge system should be visible in the UV and far UV range. A strong NO emission also exists below 300 nm (gamma band system). Atomic hydrogen originates from water molecules. Surprisingly, no Ar lines are visible whereas there is about 1% of argon in air. This fact maybe due to charge/excitation transfer reactions. Due to the low particle density and low temperature in the core of the jet [3,4,13], it is believed that light, atomic lines and molecular bands, originates mainly from recombination of ions. When moving downstream along the jet axis, the light intensity decreases quickly, however, as can also be observed in Fig. 11, the shape of the measured spectrum does not change much. The N_2^+

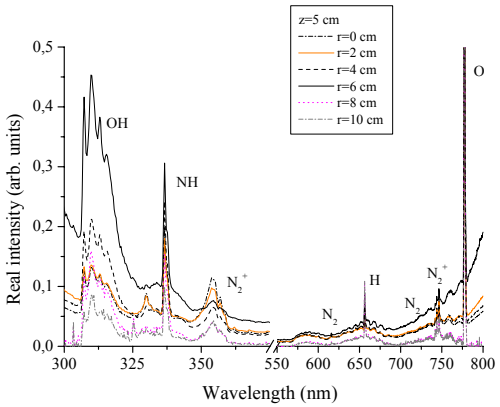

Fig. 12: Emission spectrum of an air plasma jet measured for different radial position at *z*=5 cm (160 A, 6.7 Pa), normalised to the O peak at 777 nm. Surprisingly, the NH, OH and N_2(B) quantity is largest at the jet boundary.

bands vanish owing to the efficient dissociative-recombination reaction. H* is also quickly lost. This is a strong sign in favour of a frozen chemistry (apart from *e*-ion recombination) in the sense that no new species are formed in the flow behind the nozzle. The plasma jet composition is solely determined (ignoring charged particles) by what does occur inside the dc-arc torch nozzle.

In Fig. 12, corrected air plasma emission spectra obtained for different radial positions at z=5 cm behind the nozzle outlet are plotted. The emission spectroscopy setup has been calibrated using black body radiation (W ribbon lamp for longer wavelenths and deuterium lamp for the short wavelength region). For the sake of clarity, all spectra have been normalised to the 777 nm O peak. Surprisingly, the amount of excited NH, OH and N_2(B) molecules is largest at the jet boundary (r=6 cm). Direct excitation of the molecules at the boundary is unlikely (too low T_e and n_e). This strange fact can rather be explained in terms of plasma-wall interactions. The collection of streamlines that define the jet limit originate in the

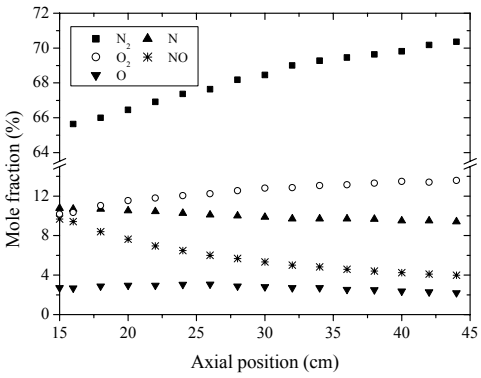

Fig. 13: Axial distribution of the neutral mole fraction in a N_2-O_2 plasma jet.

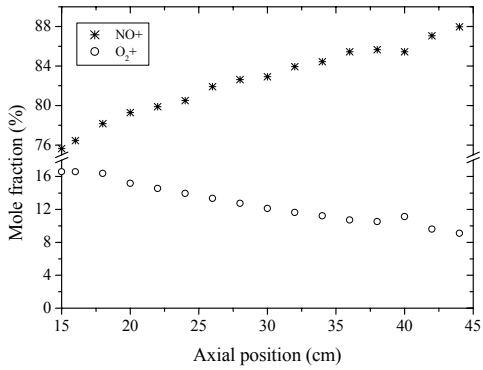

Fig. 14: Axial distribution of the two main ion mole fraction in a N_2-O_2 plasma jet.

nozzle boundary layer. We can reasonably think that many NH* and OH* and N_2* are produced at the cold nozzle copper wall via surface association processes of atomic radicals, the excess of energy being a direct consequence of the production mechanism. As there is almost no destruction during the expansion process due to the low collision frequency, molecules formed at the nozzle wall are transported in the downstrem region.

It seems that radiation mostly emanates from molecules, see Fig. 12, and strong emission of NO and O_2 below 300 nm is not taken into account, as it has been observed in shock tube experiments for shock speeds below 10 km.s^{-1} [8].

Plasma jet: mass spectrometry

The determination of the relative concentration of neutrals and ions in a N_2-O_2 free plasma jet has been carried out using a quadrupole mass spectrometer (Balzers QMG 420). Measurements have been performed with the SR1 wind-tunnel equipped with the plasma torch described in this paper under the following conditions: 100 A, 15 slm N_2-O_2, 14.3 Pa background pressure. The mass spectrometer is located in front of the plasma source at the end side of the vacuum chamber. The apparatus orifice (0.1 mm diameter) has been especially designed for minimising disturbances inside the orifice channel [14]. However, the orifice is situated in a water-cooled copper plate with a diameter of 18 cm. As a consequence, the free plasma jet is not directly sampled, the detection occurring in front of a metallic surface placed into the flow. Note that contrary to emission spectroscopy, mass spectrometry delivers information about ground-state species.

The on-axis distribution of the neutral mole fraction in a N_2-O_2 supersonic plasma jet is shown in Fig. 13. N_2 and O_2 molecules are the main constituents of the plasma, and the presence of NO is revealed. Three is no sign for the existence of a shock front (see Fig. 7) since the detection is always performed in a stagnation zone. The fraction of N_2 and O_2 molecules are relatively important.

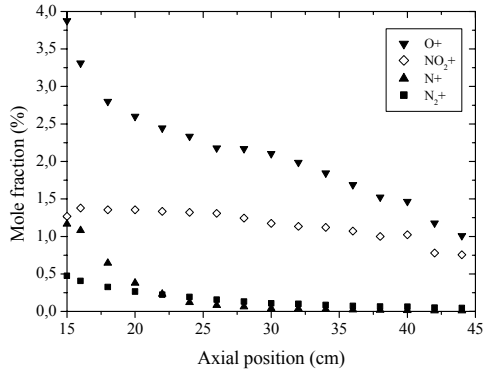

Fig. 15: Axial distribution of the minor ion mole fraction in a N_2-O_2 plasma jet.

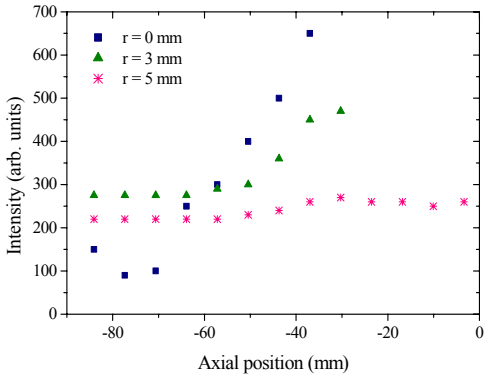

Fig. 16: 323.6 nm light emitted by OH* as a function of the distance to a metallic sphere's centre (d=7.4 cm) at floating potential plunged into a supersonic air plasma jet.

Such measured fraction may not represent the real N_2 and O_2 fraction in the free jet. Indeed, recombination of N and O atoms onto the entrance plate of the mass spectrometer to form N_2 and O_2 may not be negligible. The rise in the N_2 and O_2 mole fraction with z is certainly due to the cooling down of the flow [3]. The NO fraction decreases when the distance to the nozzle exit is increased, as can be seen in Fig. 13. This may be an indication in favour of wall-production of NO, since the chemistry is frozen in the jet. Traces of N_2O and NO_2 molecules have also been detected. Note that when adding 2% of Ar and in the case of pure N_2 plasma, no N atoms are detected.

The on-axis distribution of the ion mole fraction is shown in Fig. 14 and 15. Surprisingly, NO^+ is the main ion, whereas N_2^+, N^+ and O^+ only represent a minute fraction of the total ion content. Furthermore, the fraction of NO^+ increases whereas it is known that the charge particle content decreases in a plasma jet due to e-ion recombination [3,6] (apart from the density jump across the shock region). Another fact must be pointed out: As shown in Fig. 11, N_2^+ emits lots of light contrary to N_2 which is probably the main compound in an air plasma jet and certainly the main one in front of a plate (see Fig. 13). Therefore it must exist an efficient way of destroying resonant N_2 states.

Electron density and temperature

The electron density and temperature has been measured by means of electrostatic probes close to a stainless steel surface placed into the plasma jet (probe holder) [15]. Experimental conditions are the following: 100 A, 10 slm N_2-O_2, 13 Pa. The complete set of results can be found in [15]; we only mention here the main outcomes. When the probe is placed in the supersonic flow domain at $z = 10$ cm, one finds $n_e = 5\times10^{18}$ m^{-3} and $T_e = 7700$ K. In the subsonic domain at $z = 40$ cm, one finds $n_e = 2\times10^{17}$ m^{-3} and $T_e = 7000$ K. Recombination leads to a low electron density in the vicinity of the probe. However, remaining electrons have a high temperature. Studies that concern the electron behaviour in a supersonic plasma jet are described in [6,13]. An interesting review of all different ways of determining electron parameters in a plasma environment is presented in reference [16].

Supersonic plasma flow around a model

Generation of light in a bow shock

The light emitted by excited molecules in the vicinity of a flow body plunged into a rarefied supersonic plasma jet has been monitored [17]. In Fig. 16, the intensity of the OH* UV radiation is plotted as a function of the distance to a metal sphere's centre at floating potential for three different radial positions. The sphere is placed into the supersonic domain of an air plasma jet (100 A, 16 Pa). The light intensity, i.e. the OH* density, is maximum on the jet axis and close to the jet surface. We can think about several explanations: OH* formation from recombination of O and H atoms onto the metal surface, local dissociation of H_2O molecules, recombination of OH^+ in the boundary layer, excitation of OH due to the high temperature in the bow shock, pure compression effect. This simple example reveals the complexity of the interaction between a supersonic plasma jet and an object.

It has been observed that along the jet centreline the N_2^+ molecular ion emission drops in the vicinity of the sphere due to recombination behind the bow shock wave.

Electron temperature in the wake of a flow body

Electron parameters have also been measured in the surroundings of a metal sphere plunged into a rarefied supersonic air plasma jet (see previous section for the conditions) [17]. The electron density is highest in the bow shock wave and low in the trailing wake, as expected. As can be seen in

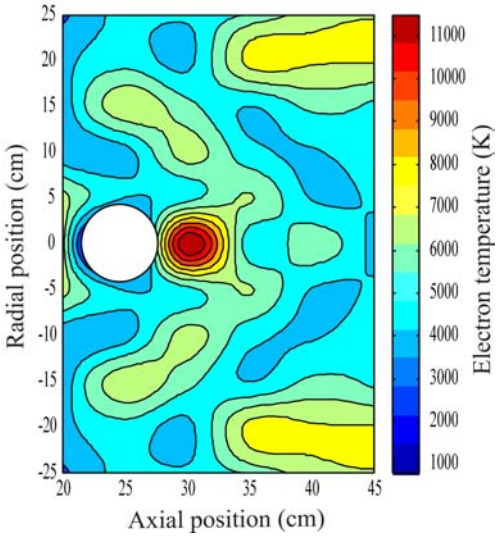

Fig. 17: Map of the electron temperature T_e around a metallic sphere plunged into the supersonic flow domain of a free air plasma jet. The high value of T_e in the wake may be a direct consequence of plasma sheath formation.

Fig. 17, the electron temperature is maximum behind the sphere, i.e. in the wake. No satisfactory explanation has yet been found. The high value of T_e in the wake may originate in the acceleration of electrons in the electric field of the plasma sheath. Low energy electrons could also be consumed during recombination processes, leaving solely intact the tail of the EEDF. Flow effects such as recirculation are unlikely at low residual pressure. Note that the mean free path is around 3 cm under our conditions. It would be interesting to verify in a near future whether the heavy particle temperature is high in the wake of the sphere. Polarisation of the sphere may also help in understanding this experimental observation. In case of space capsule or space probe, radio communication antennas are usually located at the backside, and a high electron temperature may induce transmission disturbances.

Formation of excited molecules onto surfaces

When a stainless steel sphere is placed in the vicinity of a supersonic air plasma jet (close to the jet boundary), a thin layer of faint pink light surrounds the sphere: The sphere is "glowing". Under certain experimental conditions (appropriate flow-current combination) the same light appears around the grounded torch nozzle housing. This phenomenon has also been observed in pure N_2 plasma meaning that O_2, Ar and H_2O do not play any role. Note that the light is not formed onto a non-conducting surface, as checked.

The light spectrum has been analysed using the emission spectroscopy setup previously mentioned. In Fig. 18, the emission spectrum of air plasma jet is compared to the spectrum of the light observed under identical conditions around the nozzle

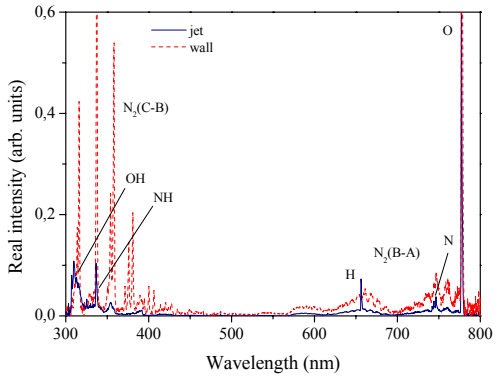

Fig. 18: Emission sprectrum of an air plasma jet (r=5 cm, z=8 cm, 160 A, 7 Pa) (solid line). Spectrum of the light observed under identical conditions around the arc-jet nozzle (dashed line). In the metallic wall vicinity, OH, NH, and N_2^+ bands vanish, the atomic line intensity decreases, the N_2 second positive system appears and the intensity of the N_2 first positive system increases. The last two points indicate a production of $N_2(C)$ and $N_2(B)$ molecules.

housing (Cu and brass have been used; both material lead to light generation). In the vicinity of the wall, OH, NH, and N_2^+ bands vanish, the atomic line intensity decreases, the N_2 second positive system (C→B transition) appears and the intensity of the N_2 first positive system (B→A transition) increases. The last two points indicate a production of $N_2(C)$ and $N_2(B)$ molecules.

The figure 19 shows a comparison between the experimental spectrum of the N_2 first positive system that corresponds to the light generated onto a metal wall and a theoretical spectrum calculated for Boltzmann equilibrium conditions with T_{rot}=1000 K and T_{vib}=8000 K (parameters corresponding to the best fitted spectrum). Overpopulation of high J and high v levels of the B state can clearly be seen in Fig 19. In other words, close to the nozzle housing metal wall N_2 molecules in the electronic B state are highly vibrationally and rotionally excited. The production mechanism of $N_2(B)$ and $N_2(C)$ molecules has not yet been clarified. However, three ways can be proposed. A production mechanism via direct electron impact on $N_2(X)$ or $N_2(A)$ molecules is possible. High-energy electrons (several eV) are needed. However, such electrons may be present if a secondary discharge is formed onto the nozzle housing as the result of current leakage from a diffuse arc. Another possible way is the excitation exchange between excited N_2 molecules like $N_2(X,v)$ and $N_2(A)$. A large quantity of $N_2(X,v)$ or $N_2(A)$ molecules is necessary to induce a detectable amount of radiation. Recombination of ground-state N atoms onto the metal wall could result in a sufficiently large quantity of the desired molecules. The last possibility is the direct association between ground-state $N(^4S)$ atoms and metastable $N(^2D,^2P)$ atoms.

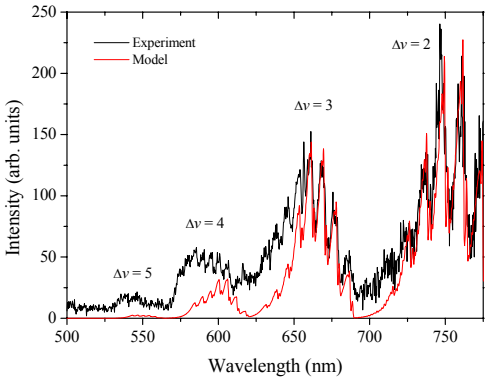

Fig 19: Measured emission spectrum of the N_2 first positive system and corresponding calculated spectrum for Boltzmann equilibrium conditions (T_{rot}=1000 K, T_{vib}=8000 K). The light originates from the surface of the arc-jet nozzle housing (air plasma, 130 A, 7 Pa). Overpopulation of high J and high v levels of the B state is obvious.

In order to be able to explain the reason for the existence of a faint pink light layer around the nozzle housing, the N_2(A) vibrational ladder must be probed and the EEDF must be measured in the surface vicinity with and without the light. The role of the background pressure must also be clarified.

Conclusions and perspectives

A rarefied supersonic plasma jets that results from the expansion of a thermal plasma into a low pressure environment can serve as a ground simulation tool for supersonic flight conditions at high altitude in the Earth's atmosphere. A high Mach number (M≈8) as well as a high temperature behind the bow shock wave (T≈8000 K) can certainly be reached. Studies carry out with such a continuous plasma wind-tunnel are complementary to shock tube and pulsed wind-tunnel experiments as only a part of the whole hypersonic flight conditions can be simulated.

In the near future, efforts will be made on numerical simulation of the plasma flow and a complete investigation of the SR5 wind-tunnel flow characteristics will be realised. Later on, research will focus on plasma-surface interaction processes behind a bow shock wave. Also of interest is the direct interaction between atomic oxygen and the vehicle surface, which is directly responsible for wear of the thermal protection, debris formation and paint flaking. Studies will be performed in Orléans with the Pelican facility [18]. A hypersonic plasma beam system, the Saphyr facility, is also currently under construction at the Laboratoire d'Aérothermique.

Acknowledgements

The authors would like to thank Prof. D.C. Schram and Dr. R. Engeln from the Eindhoven University of Technology in the Netherlands for reading the paper and for the authorisation of publishing results obtained in their research group. This work was carried out with the support of the European Community, under the Access to Research Infrastructure action of the IHP program.

References

[1] V. Lago, A. Lebéhot, M. Dudeck, S. Pellerin, T. Renault, P. Echegut, *J. Therm. Heat Transfer* **15**, 168 (2001).

[2] R. Engeln, S. Mazouffre, P. Vankan, D.C. Schram, N. Sadeghi, *Plasma Sources Sci. Technol.* **10**, 595 (2001)

[3] D.C. Schram, S. Mazouffre, R. Engeln, M.C.M. van de Sanden, in Atomic and Molecular Beams, edited by R. Campargue, Springer (2001) and references herein.

[4] S. Mazouffre, *Transport Phenomena in Plasma Expansions Containing Hydrogen*, Ph.D. Thesis, Eindhoven University of Technology (2001), available on-line at: *www.tue.nl/bib/indexen.html*

[5] S. Mazouffre, I. Bakker, P Vankan, R. Engeln, D.C. Schram, to be published in *Plasma Sources Sci. Technol*.

[6] M.C.M. van de Sanden, R. van den Bercken, D.C. Schram, *Plasma Sources Sci. Technol.* **3**, 501 and 511, (1994).

[7] S. Mazouffre, M.G.H. Boogaarts, I. Bakker, P. Vankan, R. Engeln, D. C. Schram, *Phys. Rev. E* **64**, 016411 (2001).

[8] C. Park, *J. Therm. Heat Transfer* **7**, 385 (1993).

[9] K. Fujita, S. Sato, T. Abe, Y. Ebinuma, *J. Therm. Heat Transfer* **16**, 77 (2002).

[10] G. Dilecce and S. De Benedictis, *Plasma Sources Sci. Technol*. **8**, 266 (1999).

[11] R.A. Mitcheltree, *J. Spacecraft* **28**, 619 (1991).

[12] D.A. Levin, S.F. Gimelshein, N.E. Gimelshein, *J. Therm. Heat Transfer* **16**, 251 (1995).

[13] G. Poissant, M. Dudeck, *J. Appl. Phys.* **58**, 1772 (1985)

[14] A.T. Schönemann, V. Lago, M. Dudeck, *AIAA paper* **95-1959** (1995).

[15] P . Asselin, S. Cayet, P. Lasgorceix, V. Lago, M . Dudeck, *J. Therm. Heat Transfer* **9**, 416 (1995).

[16] R.F.G. Meulenbroeks, M.F.M. Steenbakkers, Z. Qing, M.C.M. van de Sanden, D.C. Schram, *Phys. Rev. E* **49**, 2272 (1994).

[17] V. Lago, A. Lebéhot, and M. Dudeck, *Proceedings of the 36th Applied Aerodynamics Symposium,* Orléans, France (2000).

[18] A. Lebéhot, R. Campargue, *Phys. Plasma* **3**, 2502 (1996).